Available online at www.sciencedirect.com
SCIENCE DIRECT®
Thin Solid Films 451–452 (2004) 612–618
thin solid films
www.elsevier.com/locate/tsf

Hybrid solar cells based on inorganic nanoclusters and conjugated polymers

E. Arici[a,*], H. Hoppe[a], F. Schäffler[b], D. Meissner[c], M.A. Malik[d], N.S. Sariciftci[a]

[a]*Linz Institute for Organic Solar Cells (LIOS), Physical Chemistry, Johannes Kepler University, Altenberger Street 69, A-4040 Linz, Austria*
[b]*Semiconductor Physics, Johannes Kepler University Linz, Altenberger Street 69, A4040 Linz, Austria*
[c]*3 Fachhochschule Wels, Roseggerstr. 12, A-4600 Wels, Austria*
[d]*Department of Chemistry, Manchester University, Oxford Road, Manchester M13 9PL, UK*

Abstract

We investigated blends of semiconducting polymers with copper indium diselenide nanocrystals for photovoltaic applications. Depending on the synthesis, the particles are shielded by different amount of organic surfactants. Different concentrations of these nanoparticles were suspended in the polymer solutions and spin cast onto ITO glass. Solar cells were then produced by evaporation of aluminium as the back contact. Optical, electrical and morphological properties of this new prototype of composite solar cells were investigated.

Keywords: Photovoltaic; $CuInSe_2$ nanoparticles; Hybrid solar cells; Polythiophene

1. Introduction

$CuInSe_2$ (CISe) is one of the most promising materials for the fabrication of thin film solar cells due to its high absorption coefficient, suitable low band gap and radiation stability. Films of CISe have been grown by different methods such as molecular beam epitaxy [1,2], liquid-phase epitaxy [3] and halogen vapor epitaxy [4].

High efficiencies for CISe solar cells were obtained by vacuum co-evaporation methods using multistage growth processes [5]. An alternative method for efficient devices is to fabricate multilayers of Cu and In and selenize them in a second stage [6]. Deposition techniques are excellent tools for prototyping films in a small scale. On the other hand, large-scale productions by co-evaporation methods are rather challenging.

Recently a non-vacuum process have been introduced to obtain CIGaS layers on flexible large area substrates, where a thin film of the metal oxides is coated first from a solution. In a next step, the precursor film is converted into a CIGaS absorber film reducing the oxides and selenizing them afterwards using a dilute gas mixture of H_2Se and N_2 gases at 450 °C [7].

An alternative route for the low cost production may be using hybrid materials consisting of inorganic nanoparticles embedded in polymer matrices. An advantage of hybrid materials is to combine the good absorbance properties of one or more kinds of inorganic nanoparticles with the film forming properties of polymers. Most of the polymers can be processed from solution at room temperature enabling the manufacturing of large area, flexible and light weight devices.

The basic principles of hybrid solar cells are similar to the bulk heterojunction concept utilized by p-type semiconducting polymers and n-type C_{60} derivatives [8,9]. Owing to the fabrication of an interconnected network structure of p- and n-type materials in a single layer, an extremely rough interface (over the whole 'bulk') for effective charge separation has been created. The generated free charges are then transported on different phases through the device to the respective electrodes. The charge collection is dependent on how the carriers can reach the electrodes without recombining with oppositely charged carriers in the photoactive layer. Structures similar to those are fabricated by simply mixing inorganic semiconducting particles with organic clusters by spin-coating to form nanoporous semiconductor films [10].

*Corresponding author.
E-mail address: elif.arici@jku.at (E. Arici).

0040-6090/04/$ - see front matter © 2003 Elsevier B.V. All rights reserved.
doi:10.1016/j.tsf.2003.11.026

Based on interconnected networks of hole conducting polymers (p-type) with elongating n-type inorganic nanoparticles, an external quantum efficiency of 55% has been received under monochromic illumination at 485 nm with a power intensity of 0.1 mW/cm^2 [11].

N-type $CuInSe_2$ (and also $CuInS_2$)/p-type polypyrrole (PPy) heterojunctions were prepared using electrochemical techniques [12,13]. The studies showed that the deposition of thin PPy film onto $CuInS_2$ (CIS) is preferable for the device fabrication. Using bilayer device configurations of ITO/CIS/Ppy/Ag an open circuit voltage of approximately 0.5 V and a short circuit current of 6.5 mA/cm^2 have been received by an illumination of 100 mW/cm^2 intensity.

To increase the interface of p–n junctions, CIS nanoparticles should be embedded in conjugated polymers. Contrary to the organic materials, the nanocrystals are not easily dispersed in polymer matrices. Because of the small size of the cluster, they have a high surface energy, which leads easily to aggregation or to oxidation. Using an organic layer as a surfactant surrounding the nanoparticle can partly prevent such processes. On the other hand, the existence of the surfactant may also limit the performance of the hybrid devices by poor charge transport through the nanoparticle–polymer interface.

Quantized CIS nanoparticles shielded by several organic ligands have been synthesized previously [14–17]. Quantized CIS nanoparticles could be formed to homogenous layers via spin casting using triphenyl phosphite (TPP) as a surfactant [18]. The monolayers of quantized CIS/TPP show photovoltaic activity, after an annealing process at only 120 °C. Heterostructures of CIS/TPP with small organic molecules have been carried out [18]. In a double layer configuration, consisting of a good soluble C_{60} derivative [19,20] (1-(3-methoxycarbonyl)-propyl-1-1-phenyl-(6,6)C_{61}) as hole blocking layer, a promising cell performance has been reported. Illuminating the cell with 80 mW/cm^2 white light from a solar simulator produced an open circuit voltage V_{oc} of 710–790 mV and a short circuit current density of approximately 0.26 mA/cm^2. Replacing the CIS/TPP single layer by a blend of CIS/TPP and highly p-doped poly(ethylene dioxythiophene) (PEDOT:PSS) in the same bilayer configuration lead to an increase of the quantum efficiency up to 20% [21].

A further optimization of the photovoltaic response in CIS hybrid systems may be achieved by surface modification, so that a dispersion of the nanoparticles in toluene is possible. This property would open the door to prepare blends of nanoparticles with conjugated polymers, which are the subject of organic photovoltaic devices. Contrary to PEDOT:PSS, poly-hexylthiophene (P3HT) for example, has the advantage that it absorbs in the visible range and may contribute to the charge creation in the bulk [22,23]. Additionally, an increase of the average nanoparticle size above the Bohr exciton radius (≈10 nm) of the bulk material would suppress the size quantization effects and lead, therefore, to a broader absorbance. In this contribution, we considered the synthesis strategies fulfilling the requirements above and report the first investigations on CISe–P3HT blends as photovoltaic materials. One finding described above in more detail was that not only the chemical structure but also the amount of the surfactant is a critical parameter for the device morphology and performance.

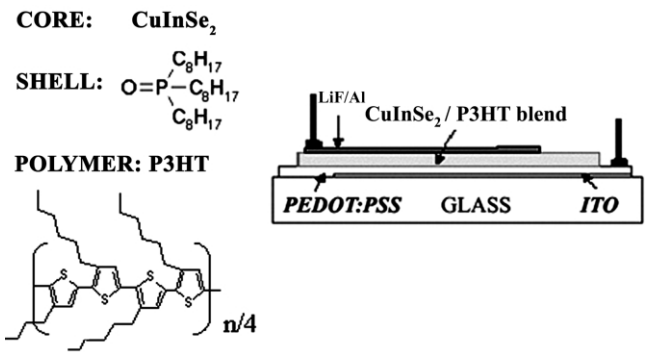

Fig. 1. Materials used in $CuInSe_2$/P3HT bulk heterojunction solar cells.

2. Experimental

2.1. Materials

The materials investigated are shown in Fig. 1. P3HT is commercially available from Aldrich. Synthesis of $CuInSe_2$ particles has been performed by using hot injection method [17]. In this synthesis, the CISe particles are shielded by an organic surfactant tri-*n*-octyphoshine oxide (TOPO) against environmental influences. Se, TOPO, indium (III) chloride were purchased from Aldrich Chemical Company. TOPO was purified by vacuum distillation at 250 °C.

Synthesis of TOPO-capped $CuInSe_2$ nanoparticles:

A mixture of Se powder (1.70 g) and tri-*n*-octyphoshine (TOP) (15 ml) was stirred at room temperature and under inert gas atmosphere for 24 h to give a transparent solution of TOPSe. A solution of $InCl_3$ (0.01 mol) and CuCl (0.01 mol) in TOP was injected into TOPO at 100 °C. After stirring the reaction mixture at 100 °C for 1 h, the temperature was increased to 330 °C at which point TOPSe was injected into the reaction mixture. A colour change from yellow to black occurred spontaneously. After 30 min, the reaction mixture was cooled to 80 °C and an excess of methanol added into it. A flocculate of nanoparticles formed which was separated by centrifugation. The nanoparticles were washed three times with methanol to remove any excess TOPO and other organic impurities and resuspended in toluene for further investigations.

2.2. Cell preparation and experimental methods

Absorption studies were carried out using a HP 8453 spectrometer.

Blends of CISe and P3HT were prepared from an approximately 3 wt.% toluene solution by spin coating onto ITO glass (supplied by BALZER). Film thickness in the order of 200 ($\pm$30) nm was obtained this way. Aluminum (300 nm) was evaporated as counter electrode on the films.

The spin-cast parameter of the percolated blends [23] consisting n-type methanofullerene and P3HT has been adapted to CISe/P3HT blends. The volume of a $CuInSe_2$ molecule, with the ionic radius of Cu ~ 0.096 nm, In ~ 0.081 nm and Se ~ 0.198 nm, has been roughly estimated to be 2/3 of a methanofullerene molecule. Therefore, a weight ratio of 4.5:1 for CISe:P3HT mixtures may be the lower limit to prepare percolated films. The amount of CISe was varied in the blends below and above the estimated limit and the effect on photovoltaic parameter was measured after an annealing process of the blends for 2 h at 150 °C under vacuum.

Current–voltage (I–V) measurements were performed at room temperature in argon using a Keithley 617 source-monitor unit. For electrical characterization the cells were illuminated with 80 mW/cm^2 power intensity of white light by a Steuernagel solar simulator (active area to ~5–6 mm^2) by the size of back electrode. The filling factor FF was calculated by $FF = V_p \times I_p / (V_{oc} \times I_{sc})$ with V_p and I_p being the voltage and current of the maximum power point and V_{oc} and I_{sc} the open circuit voltage and the short circuit photocurrent, respectively.

The crystallographic structure of the product was determined by powder X-ray diffraction (XRD) using Cu Kα radiation of 1.5418 Å. The scan rate of 0.1°/s was applied to record the patterns in the 2θ range of 10–60°.

The size of the prepared CISe nanoparticles was studied by transmission electron microscopy on a Jeol 2012 FasTEM at 200 kV.

3. Results and discussion

3.1. Material properties of TOPO-capped $CuInSe_2$

We investigated first the crystallographic structure of the TOPO-capped CISe by powder XRD. Additionally, the amorphous contribution of TOPO was detected as a function of the sample history. The XRD patterns of $CuInSe_2$ nanoparticles are displayed in Fig. 2.

The main difference of sample preparation was the time, the sample was left in excess of methanol to wash away the organic impurities as described in Section 2. Sample A have been washed in MeOH just for 10 min, sample B for 40 min.

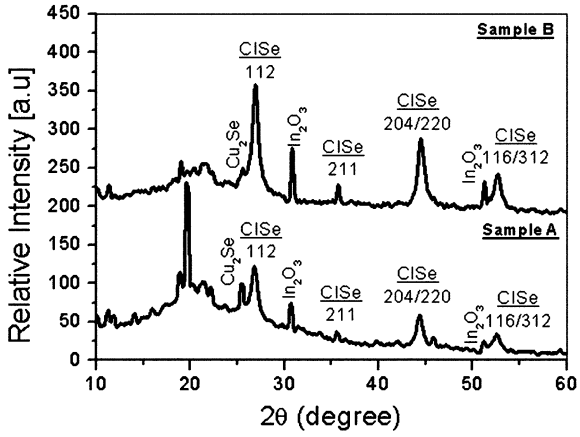

Fig. 2. XRD patterns of CISe nanocrystals with different sample history shown in arbitrary units. Sample A have been washed in MeOH for 10 min to remove the organic surfactants (sample B for 40 min).

An intense peak at 2θ = 27.0° oriented along the (1 1 2) direction and other prominent peaks observed at 44.6° ((2 2 0)/(2 0 4)) and 52.7° ((3 1 2)/(1 1 6)) indicate the chalcopyrite structure of $CuInSe_2$ (Fig. 2). In addition to these, weak orientations at 30.9°, 51.1° and 60.9° are also observed. The presence of these peaks may be due to the existence of by-products Cu_2Se and In_2O_3. During the wash-process including centrifuging afterwards, most of the by-products have been removed. The intensity of the by-product peaks for sample B is lower than that for the case of sample A.

Important are also the changes at the 2θ range between 15° and 35° depending on the sample history. Because of the given synthesis conditions, the organic surfactants TOP and TOPO, which are acting also as solvents during the reaction, exist in an excess amount in the product. Owing to their amorphous contribution to the diffractogramm, a broad halo appears in the 2θ ranges of 15° and 35°. A comparison between the sample A and B shows that the intensity of the broad halo is lower for sample B, so that we can conclude that the excess amount of the surfactants has been partly removed by washing process.

Next, we consider the size and shape of the CISe nanoparticles by high-resolution transmission electron microscopy (HRTEM). Fig. 3 displays the HRTEM image of a single CISe nanoparticle with dimensions of approximately 15 nm × 20 nm. The shape of the investigated nanograins was mostly sharp-edged, rather than spherical. It is sufficient to point out here that qualitatively similar results were obtained also for concentrated films. CISe particles revealed a narrow size and shape distribution.

The electron diffraction patterns in Fig. 3 show broad reflection spots, which may indicate the polycrystallinity of the product. Broadening of the diffraction pattern could also result from the overlap of many nanoparticles

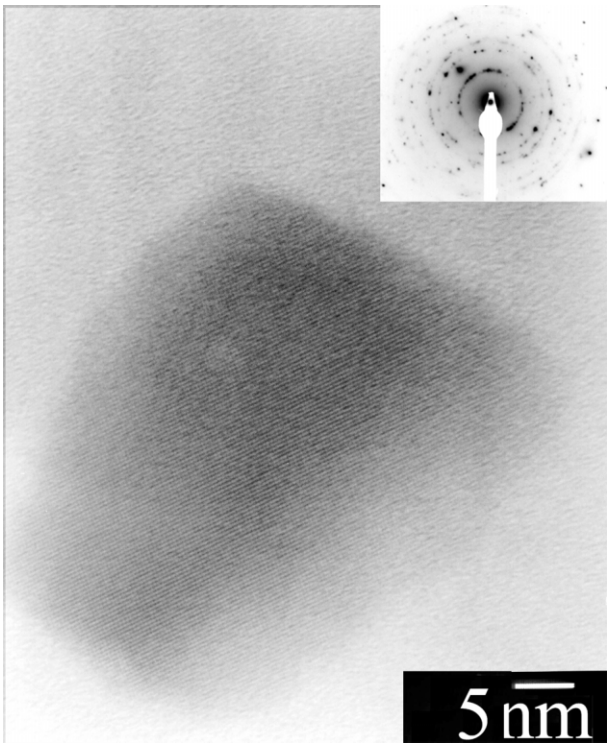

Fig. 3. HRTEM images of TOPO-shielded CISe particles. Selected-area electron diffraction patterns of the nanoparticles show the presence of polycrystalline nanostructures with the characteristic broad reflections.

with different orientations. Inductively coupled plasma atomic emission spectroscopy analysis (Cu, In, Se) of the nanoparticles shows the composition to be $Cu_1In_1Se_2$.

3.2. Material properties of $CuInSe_2$-polymer blends

Tapping mode atomic force microscopy (AFM) was employed to gain insight into the structure of the different CISe/P3HT mixtures. In general, the AFM studies show that the interactions between the polymers soluble in toluene and the TOPO-capped nanoparticles are attractive enough to avoid a large-scale phase separation. Our finding thus seems to be in agreement with the effect reported in Ref. [24]. On the other hand, it reveals that the quality of the TOPO-capped CISe:P3HT films depends strongly on the amount of the surfactant. According to the X-ray investigations, shown in Fig. 2, CISe that have been washed in methanol for a shorter time has a higher amount of the surfactant. We prepared two films via spin-coating using toluene dispersions of a 10:1 wt.% CISe:P3HT mixtures, whereas the surfactant amount of the CISe was varied. Both films have been annealed at 150 °C for 2 h under vacuum.

The morphology of the film prepared from a TOPO 'rich' dispersion is displayed in Fig. 4a. The film is partly homogenous with a roughness of approximately 20–40 nm. But there are also pin holes on the film surface with diameters of approximately 0.5 μm, which are probably formed during the annealing process due to the removal of TOPO and toluene rests in the film. Consequently, the photovoltaic devices prepared from these layers were influenced by an ohmic contribution (not shown here).

CISe have been washed in methanol for 30 min longer, and consists of less TOPO considered by the weak amorphous contribution to the X-ray diffractogramm in Fig. 2. The topology of the P3HT blends prepared using the TOPO 'poor' CISe reveals a smooth surface with a roughness of approximately 50 nm and a homogenous morphology (Fig. 4b). The films are almost pin-hole free. Accordingly, for the photovoltaic characterization, films have been characterized only by using a thoroughly washed CISe sample.

In comparison to purely P3HT films, the film transparency was rather low, especially for the films, which contain CISe with a short-time washing procedure. Fig. 5 shows the optical absorbance spectra of the solutions of CISe and P3HT in toluene. The absorption of CISe

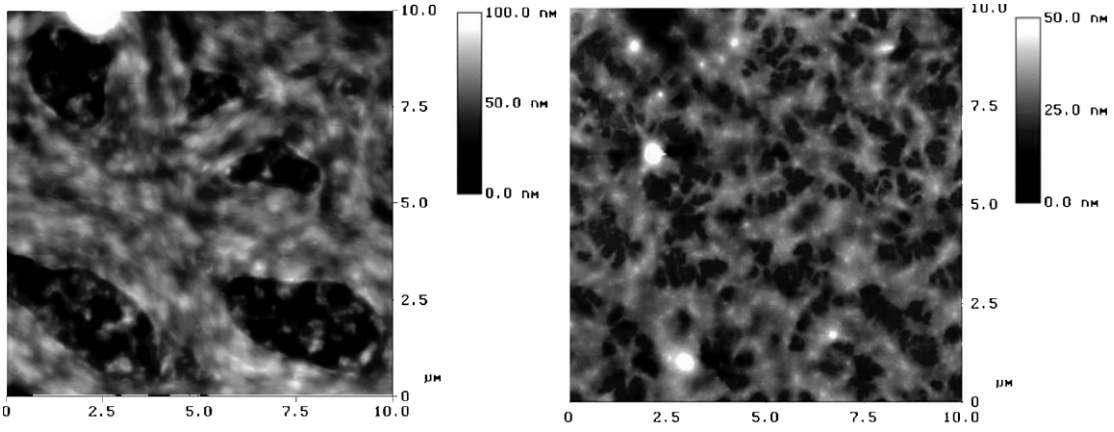

Fig. 4. AFM images of blends consist of CISe:P3HT in a weight ratio of 10:1 depending on the CISe preparation (see also Fig. 2).

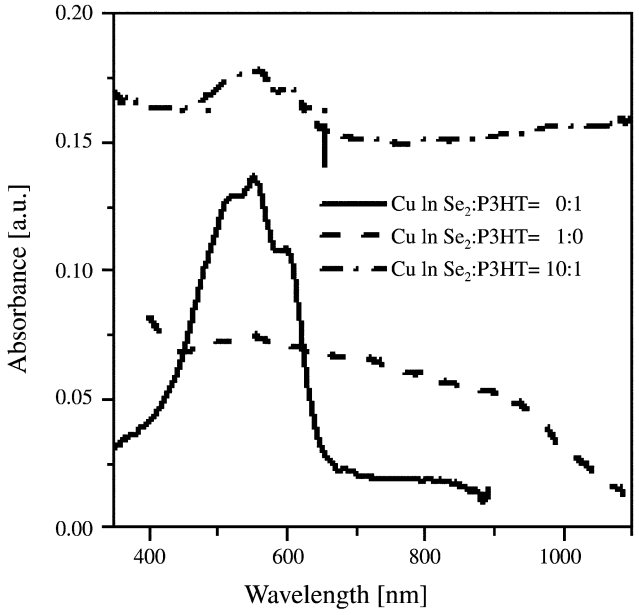

Fig. 5. Optical absorbance spectra of CISe and P3HT absorbance in toluene solution in comparison to the absorbance of hybrid films consist of CISe:P3HT in a weight ratio of 10:1.

is in a broad range of 400–1100 nm and exhibits an edge located at 947 nm. P3HT, on the other hand, shows an absorption maximum at 556 nm. The absorbance spectrum of the CISe:P3HT blends in a weight ratio of 10:1 is simply given by the superposition of the two components. There are no additional absorbance bands indicating ground state interactions between the two components. Owing to the broad absorbance of CISe, the hybrid material allows a maximum light harvesting.

The I–V characteristics of the ITO/P3HT/Al photovoltaic devices in dark and under 80 mW white light illumination have been measured under argon (Fig. 6a). In the case of a negative applied bias, i.e. positive contact to the Al and negative contact to the ITO, these devices delivered a rectification ratio of 77 in the dark at ± 2 V and 92 under illumination. There was no detectable photovoltaic effect.

Three samples with different amount of CISe particles in P3HT have been compared in their photovoltaic response. The sample consisting of 75 wt.% CISe (CISe/P3HT: 3/1) is estimated to be below the percolation threshold (Section 2.2). Two additional samples with 85 and 90 wt.% CISe should be above the critical value for the percolation.

By white light illumination of an ITO/CISe–P3HT/Al cell (CISe/P3HT: 3/1) with a power intensity of 80 mW/cm^2, we received open circuit voltages V_{oc} of 0.65–0.70 V and short circuit current densities I_{sc} of 20–30 μA/cm^2 (Fig. 6b). The calculated fill factor of the diode is 0.42. The rectification ratio in the dark is 12 at ± 2 V and 16 under illumination.

A remarkable approach to enhance the photovoltaic properties was using percolated blends of CISe–P3HT in a weight ratio of 6:1 in the same cell design. These devices delivered a short circuit current of 0.3 mA/cm^2 and an open circuit voltage of 1 V. From sample to sample, there were differences for the I_{sc} values in a range of 0.2–0.3 mA and for the V_{oc} values in a range of 0.75–1 V (Fig. 6c). The rectification ratio in the dark is 7 and 5.3 under illumination at ± 2 V. The calculated fill factor of the diode is 0.5.

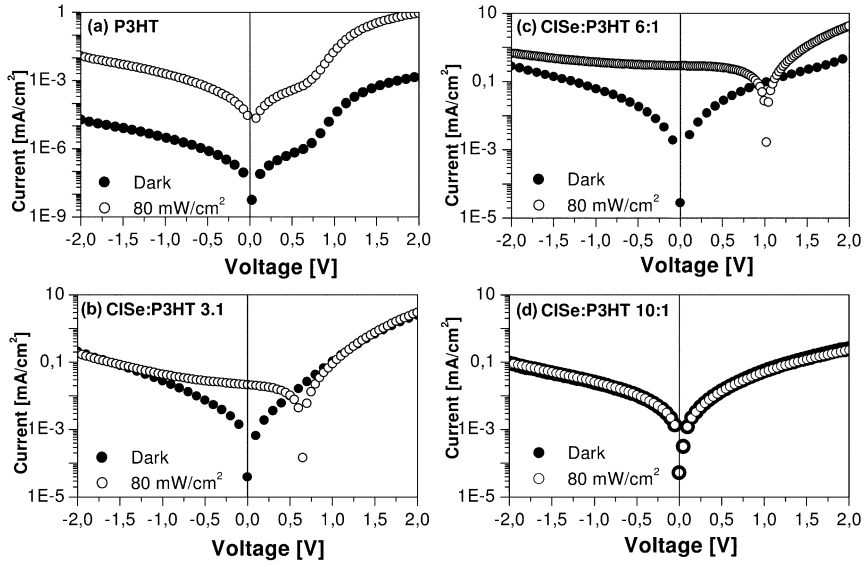

Fig. 6. I/V characteristics of P3HT/CISe hybrid devices with increasing CISe amount in comparison to pure P3HT devices in the dark and under AM 1.5 illumination.

A further increasing of the CISe amount in the polymer to a weight ratio of 90% in the same cell design results in a decreasing of the rectification ratios 2.6 in the dark at ± 2 V and 2.75 under illumination. And there was no detectable photovoltaic effect (Fig. 6d).

A possible explanation for the increasing photocurrent in devices consisting of 85 wt.% CIS may be due to the forming of an interconnected network of the P3HT with the CISe nanoparticles. From the spectral response of the blends at wavelengths greater than 650 nm, where the CISe nanoparticles are excited exclusively, it can be inferred that the excitation of the CISe contributes to the photocurrent generation. For the sake of the evaluation of the photocurrent data, which is detected with an equipment configured for the spectral ranges up to 750 nm, complementary measurements have to be investigated.

A comparison between Fig. 6(2), (3) and (4) shows the influence of the CISe–TOPO amount in the series resistance of the device. In the dark, the influence of the series resistance can be seen in the forward direction, the curves became flat and the injection currents are lower, with increasing CISe–TOPO ratio. Accordingly, the rectification ratios became lower. Hybrid materials are three component systems including the surfactant TOPO, which is an isolator. The performance of nanocrystal-based devices might be limited by poor charge transport through the nanoparticle–polymer interface, since an increase of the CISe amount in the polymer matrix may lead also to an increase of the surfactant in the device. When the concentration of the surfactant is above a critical value, the serial resistance might be so high (Fig. 6(4)) that the charge transport is suppressed.

4. Conclusions

TOPO-capped CISe have been synthesized by thermal decomposition method. TEM investigations show that the size of the nanoparticle is approximately 15×20 nm^2 and do not show size quantization effects, so that light harvesting in a broad range should be possible. Homogenous films based on CISe and P3HT have been prepared by spin-coating, where the influence of the surfactant on the morphology has been demonstrated via AFM investigations. Films consisting of CISe:P3HT in a weight ratio of 6:1 show a significantly better photovoltaic response in comparison to P3HT single layer. These devices delivered a short circuit current of 0.3 mA/cm^2 and an open circuit voltage of approximately 1 V, when sandwiched between ITO and Al electrodes.

As a next step, we will work on optimizing existing approaches, as well as developing new procedures, in order to modify the surface properties of nanoparticles. It is possible to remove the surfactant further by repeated washing with organic solvents, providing a better charge carrier exchange between nanoparticle and the conducting polymer. Another strategy is combining surfactants, with different strength of the adsorption on the particle surface, so that the interface between the nanoparticle and the polymer can be optimized.

The X-ray, morphology and electrical characterization should be done systematically, depending on the synthesis conditions, to find a good balance between the three components to fulfill the requirements for an effective cell.

Acknowledgments

This work is sponsored by the Deutsche Bundesministerium für Bildung und Forschung, Förderkennzeichen 01SF0026. We express our sincere thanks to P. Skabara, Inorganic Chemistry, Manchester University, England. TEM work was performed at the *Technische Service Einrichtung* (TSE) of the Johannes Kepler University in Linz.

References

[1] V.K. Kapur, M. Fischer, R. Roe, Mater. Res. Soc. Symp. Proc. 668 (2001) H2.6.
[2] J.F. Guillemoles, P. Cowache, A. Lusson, K. Fezza, F. Boisivon, J. Vedel, D. Lincot, J. Appl. Phys. 79 (1996) 7293.
[3] M.E. Beck, M. Cocivera, Thin Solid Films 272 (1996) 71.
[4] T. Negami, Y. Hoshimoto, M. Nishitani, T. Wada, Sol. Energy Mater. Sol. Cells 49 (1997) 343.
[5] M.A. Contreras, B. Egaas, K. Ramanathan, J. Hiltner, A. Swartzlander, F. Hasoon, R. Noufi, Prog. Photovolt. 7 (1999) 311.
[6] K. Kushiya, Thin Solid Films 387 (2001) 257.
[7] V.K. Kapur, A. Bansal, P. Le, O.I. Asensio, Thin Solid Films 431–432 (2003) 53.
[8] C.J. Brabec, N.S. Sariciftci, J.C. Hummelen, Adv. Funct. Mater. 1 (2001) 15.
[9] S. Shaheen, C.J. Brabec, F. Padinger, T. Fromherz, J.C. Hummelen, N.S. Sariciftci, Appl. Phys. Lett. 78 (2001) 841.
[10] C. Stalder, J. Augustynski, J. Electrochem. Soc. 126 (1979) 2007.
[11] W.U. Huynh, J.J. Dittmer, A.P. Alivisatos, Science 295 (2002) 2425.
[12] S. Bereznev, J. Kois, E. Mellikov, A. Öpik, D. Meissner, $CuInSe_2$/Polypyrrole photovoltaic structure prepared by electro-deposition presented at 17th European Photovoltaic Solar Energy Conference, Munich, Germany, October 22–26, 2001.
[13] S. Bereznev, I. Konovalov, J. Kois, E. Mellikov, A. Oepik, MRS Symposium Proceedings, 771, 243–248, 2003.
[14] C. Czekelius, M. Hilgendorff, L. Spanhel, I. Bedja, M. Lench, G. Müller, U. Bloeck, D. Su, M. Giersig, Adv. Mater. 11 (1999) 643.
[15] E. Arici, H. Hoppe, A. Reuning, N.S. Sariciftci, D. Meissner, CIS Plastic Solar Cells 17th European Photovoltaic Solar Energy Conference, Proceedings of the International Conference held in Munich, Germany, 2001.
[16] B. Li, Y. Xie, J. Huang, Y. Qian, Adv. Mater. 11 (1999) 1456.

[17] M.A. Malik, N. Revaprasadu, P. O'Brien, Adv. Mater. 11 (1999) 1441.
[18] E. Arici, N.S. Sariciftci, D. Meissner, Mol. Cryst. Liq. Cryst. 383 (2002) 129.
[19] C.J. Brabec, F. Padinger, N.S. Sariciftci, J.C. Hummelen, J. Appl. Phys. 85 (1999) 6866.
[20] C.J. Brabec, F. Padinger, J.C. Hummelen, R.A.J. Janssen, N.S. Sariciftci, Synth. Met. 102 (1999) 861.
[21] E. Arici, N.S. Sariciftci, D. Meissner, Adv. Funct. Mater. 13 (3) (2003) 165.
[22] J.J. Dittmer, E.A. Marseglia, R.H. Friend, Adv. Mater. 12 (2000) 1270.
[23] F. Padinger, R.S. Rittberger, N.S. Sariciftci, Adv. Funct. Mater. 13 (2003) 1.
[24] N.C. Greenhem, X. Peng, A.P. Alivisatos, Phys. Rev. B 54 (24) (1996) 17828.